A Metabolomics Profiling of Glaucoma Points to Mitochondrial Dysfunction, Senescence, and Polyamines Deficiency

Stéphanie Leruez,[1,2] Alexandre Marill,[2] Thomas Bresson,[2] Grégoire de Saint Martin,[2] Adrien Buisset,[2] Jeanne Muller,[2,3] Lydie Tessier,[4] Cédric Gadras,[4] Christophe Verny,[3] Philippe Gohier,[2] Patrizia Amati-Bonneau,[1,4] Guy Lenaers,[1] Dominique Bonneau,[1,4] Gilles Simard,[4,5] Dan Milea,[6] Vincent Procaccio,[1,4] Pascal Reynier,[1,4] and Juan Manuel Chao de la Barca[1,4]

[1]Equipe Mitolab, Institut Mitovasc, Centre National de la Recherche Scientifique 6015, Institut National de la Santé et de la Recherche Médicale (INSERM) U1083, Université d'Angers, Angers, France
[2]Département d'Ophtalmologie, Centre Hospitalier Universitaire, Angers, France
[3]Département de Neurologie, Centre Hospitalier Universitaire, Angers, France
[4]Département de Biochimie et Génétique, Centre Hospitalier Universitaire, Angers, France
[5]INSERM U1063, Université d'Angers, Angers, France
[6]Singapore Eye Research Institute, Singapore National Eye Centre, Duke-NUS, Singapore

Correspondence: Pascal Reynier, Département de Biochimie et Génétique, Centre Hospitalier Universitaire, 4 rue Larrey, Angers F-49933, France; pareynier@chu-angers.fr.

PR and JMCB contributed equally to the work presented here and should therefore be regarded as equivalent authors.

Submitted: May 31, 2018
Accepted: August 4, 2018

Citation: Leruez S, Marill A, Bresson T, et al. A metabolomics profiling of glaucoma points to mitochondrial dysfunction, senescence, and polyamines deficiency. *Invest Ophthalmol Vis Sci*. 2018;59:4355–4361. https://doi.org/10.1167/iovs.18-24938

Purpose. To determine the plasma metabolomic signature of primary open-angle glaucoma (POAG).

Methods. We compared the metabolomic profiles of plasma from individuals with POAG (n = 36) with age- and sex-matched controls with cataract (n = 27). A targeted metabolomics study was performed using the standardized p180 Biocrates Absolute IDQ p180 kit with a QTRAP 5500 mass spectrometer. Multivariate analyses were performed using principal component analysis (PCA) and the least absolute shrinkage and selection operator (LASSO) method.

Results. Among the 151 metabolites accurately measured, combined univariate and multivariate analyses revealed 18 discriminant metabolites belonging to the carbohydrate, acyl-carnitine, phosphatidylcholine, amino acids, and polyamine families. The metabolomic signature of POAG points to three closely interdependent pathophysiologic conditions; that is, defective mitochondrial oxidation of energetic substrates, altered metabolism resembling that observed in senescence, and a deficiency in spermidine and spermine, both polyamines being involved in the protection of retinal ganglion cells.

Conclusions. Our results highlight a systemic and age-related mitochondrial defect in the pathogenesis of POAG.

Keywords: glaucoma, metabolomics, mitochondrial dysfunction, primary open-angle glaucoma

Glaucoma is a group of chronic optic neuropathies characterized by progressive loss of retinal ganglion cells, presence of cupped optic neuropathy, and irreversible loss of the visual field.[1] This disease, affecting almost 65 million people worldwide, is the most frequent cause of irreversible blindness.[2–4] Primary open-angle glaucoma (POAG), the most common form of glaucoma, is defined by the presence of a glaucomatous optic neuropathy without an identifiable cause. The pathogenesis of POAG is multifactorial and remains to be elucidated. Principal risk factors are old age and elevated IOP, with systemic, environmental and genetic factors, high myopia, as well as sex and ethnic origins also contributing to the disease.[1] At the pathophysiologic level, in addition to increased IOP, multiple mechanisms leading to retinal ganglion cell (RGC) loss have been implicated. These include glutamate excitotoxicity, ischemia-hypoxia, dysimmunity and altered inflammatory cytokines, the influence of glial cells, trophic insufficiency due to blockade at the lamina cribrosa, oxidative stress, and mitochondrial dysfunction.[5–7]

Despite its promising statistical power to uncover new pathophysiologic biomarkers, metabolomics only rarely has been applied to POAG to date.[8,9] Indeed, this approach, combining multiple small-molecule analysis with mathematic modeling, can reveal the direct or indirect metabolic fingerprints of a disease. In comparison with other "omics" techniques, metabolomics produces profiles closer to the phenotype of the disease, integrating several other factors in addition to the genetic factors. These include the effects of age, way of life, nutrition, physical activities, medication, and so forth. However, in contrast with the genome and transcriptome that are now fully analyzable, currently available techniques of metabolomics offer only a partial analysis of the metabolome, showing specific groups of metabolites according to the approach used. The human metabolome is estimated to contain more than 110,000 metabolites (available in the public domain at http://www.hmdb.ca/) with highly variable molecular structures, but the most performant metabolomic pipeline can analyze only a few hundred metabolites at a time.

To date, to our knowledge only two metabolomic studies have been performed on the blood of individuals with glaucoma.[10] The first study compared the plasma metabolome of individuals with POAG ($n = 72$) to that of controls ($n = 72$), using high resolution mass spectrometry.[11] This untargeted metabolomic approach revealed 41 discriminant metabolites including palmitoyl-carnitine, hydroxy-ergocalciferol, sphingolipids, other vitamin D-related molecules and terpenes; thus, indicating perceptible alterations of the blood during fatty acid metabolism, steroid biosynthesis, and sphingolipid metabolism.

The second study compared the metabolome of the serum of individuals with primary angle-closure glaucoma (PACG; $n = 38$) to that of controls ($n = 48$), using gas chromatography-mass spectrometry (GC-MS).[12] This study revealed significant differences in the blood of free fatty acids, including palmitoleic, linoleic, γ-linoleic, adrenic, and arachidonic acids, the concentration of these metabolites being correlated with the level of ocular pressure.

The metabolomics of the aqueous humor in a rat model of glaucoma, induced by a series of intracamerular sodium hyaluronate injections, also has been studied using nuclear magnetic resonance (^{1}H-NMR).[13] The major discriminant metabolites identified, by decreasing order of importance, were glucose, creatine/creatinine, citrate, glutamine, fatty acids, acetoacetate, proline, glutamate/glutamine, acetate, lysine, alanine, cholesterol, valine, and very low density lipoprotein (VLDL); thus, indicating the altered metabolism of glucose, lipid, and amino acids, as well as the potential toxicity of increased glutamate concentrations for RGCs.

We used a standardized targeted metabolomic approach to compare the plasma metabolome of individuals with POAG to that of age- and sex-matched cataract controls, to further pursue the deciphering of the metabolic fingerprint of POAG.

Materials and Methods

Ethics Statement

Participants were included after having given their informed written consent for the research. The study, conducted in accordance with the ethical standards set forth in the Declaration of Helsinki (1983), was approved by the University of Angers ethical review committee (CPP OUEST 2, agreement number: CB 2013-04).

Study Participants

Individuals were recruited from the Department of Ophthalmology of Angers University Hospital, France. POAG was diagnosed based on consensual criteria; that is, glaucomatous optic nerve damage associated with increased IOP (> 21 mm Hg), and progressive optic disc cupping.[14] All included POAG patients had elevated IOP at the initial diagnosis, as well as open iridocorneal angles as determined by gonioscopic examination. Patients with isolated ocular hypertension, normal tension glaucoma, or any secondary form of glaucoma were excluded from this study. Standard automated perimetry (Humphrey field analyzer; Carl Zeiss Meditec, Dublin, CA, USA) with the 24-2 SITA Fast algorithm was performed on all POAG patients, and visual field mean defect (VF-MD) values were used to grade the severity of POAG as "mild" (<–6 dB), "moderate" (–6 to –12 dB), and "severe" (>–12 dB; perimetric Hoddap-Parrish-Anderson criteria). The reliability indices retained were false-positive or false-negative rates <15%, and fixation losses <20%. Other additional tests performed on patients with POAG included evaluation of the retinal nerve fiber layer (RNFL) thickness using spectral domain optical coherence tomography (OCT) and measurement of the central corneal thickness (CCT; Cirrus OCT, Carl Zeiss Meditec). The best-corrected visual acuity was measured using the decimal Monoyer charts, with the results converted into logMAR units for statistical analysis. IOPs were measured using the Goldmann applanation tonometer. History of glaucoma treatment was documented.

Control subjects were sex- and age-matched individuals selected among patients undergoing cataract surgery at the same department of ophthalmology. Inclusion criteria were visual acuity ≥20/50 and absence of any other associated ocular conditions except for cataract. Exclusion criteria were based on personal reasons or a family history of glaucoma, ocular hypertension, or any other intraocular pathology, including retinal disorders. The control group ($n = 27$) was age- and sex-matched with the POAG group ($n = 36$) patients.

Sample Collection

Fasting blood samples, at least 3 hours after the last meal, were collected in heparin tubes at the department of ophthalmology, rapidly transported in crushed ice to the Hospital Biological Resources Center, and immediately centrifuged for 10 minutes at 3000*g* at +4°C before recovery of the supernatant (plasma), which was conserved at –80°C in 500 µL aliquots until metabolomics analysis.

Metabolomics Analysis

Targeted quantitative metabolomics analyses were performed using the Biocrates Absolute IDQ p180 kit (Biocrates Life Sciences AG, Innsbruck, Austria). Used with mass spectrometry (QTRAP 5500; SCIEX, Villebon-sur-Yvette, France), this kit allows quantification of up to 188 different endogenous molecules distributed as follows: free carnitine (C0), 39 acylcarnitines (C), the sum of hexoses (H1), 21 amino acids, 21 biogenic amines, and 105 lipids. The lipids are distributed in the kit in four different classes: 14 lysophosphatidylcholines (lysoPC), 38 diacyl-phosphatidylcholines (PC aa), 38 acyl-alkyl-phosphatidylcholines (PC ae), and 15 sphingomyelins (SM). The full list of individual metabolites is available in the public domain at http://www.biocrates.com/products/research-products/absoluteidq-p180-kit. Flow injection analysis coupled with tandem mass spectrometry (FIA-MS/MS) was used for analysis of carnitine, acylcarnitines, lipids and hexoses. Liquid chromatography (LC) was used for separating amino acids and biogenic amines before quantitation with mass spectrometry.

All reagents used in this analysis were of LC-MS grade and purchased from VWR (Fontenay-sous-Bois, France) and Merck (Molsheim, France). Sample preparation and analysis were performed following the Biocrates Kit User Manual. Briefly, each plasma sample was thoroughly vortexed after thawing and centrifuged at 4°C for 5 minutes at 5000*g*. Then, 10 µL of each sample were added to the filter on the upper wells of the 96-well plate. Metabolites were extracted and derivatized for quantitation of amino acids and biogenic amines. The extracts finally were diluted with MS running solvent before FIA- and LC-MS/MS analysis. Three quality controls (QCs) composed of human plasma samples at three concentration levels of low (QC1), medium (QC2), and high (QC3) were used to evaluate performance of the analytical assay. A seven-point serial dilution of calibrators was added to the 96-well plate of the kit to generate calibration curves for quantification of amino acids and biogenic amines.

Statistical Analysis

Univariate analysis of clinical data was performed using the bilateral Student's *t*-test, with differences considered significant at $P \leq 0.05$.

Table 1. Demographic Data and Comorbidity Status of Individuals With POAG Compared to Controls

	POAG ($N = 36$)	Controls ($N = 27$)	*P* Values
Average age, y	72.00	73.04	0.51
Females, %	58.33	44.44	0.28
Mean BMI, kg/m^2	24.84	27.49	<0.01*
Diabetes, %	5.88	3.70	0.70
Hypertension, %	44.44	62.96	0.15
Hyperlipidemia, %	19.44	25.93	0.55
Thyroid disease, %	19.44	11.11	0.36

* Statistically significant.

Table 2. Systemic Medication of Individuals With POAG Compared to Controls

	POAG ($N = 36$)	Controls ($N = 27$)	*P* Values
Antihypertensives, %	44.44	66.66	0.08
Lipid-lowering medications, %	19.44	25.93	0.55
Antiplatelet therapy/oral anticoagulation drugs, %	13.88	29.63	0.15
Oral diabetes medications, %	11.11	7.41	0.62
Insulin, %	2.78	3.70	0.84
Corticosteroids, %	0	7.41	0.16
Thyroid hormone, %	16.67	11.11	0.53
Estrogen, %	2.78	3.70	0.84
Vitamin D, %	5.55	18.52	0.14
Others, %	38.90	55.55	0.19

Before statistical analysis, the raw metabolomics data were examined to exclude metabolites with >20% concentration values below the lower limit of quantitation (LLOQ) or above the upper limit of quantitation (ULOQ).

Univariate analysis of metabolomics data was performed using the nonparametric Mann-Whitney-Wilcoxon test (hereinafter referred to as the Wilcoxon test) for quantitative variables and Fisher's exact test for qualitative variables. The Benjamini-Hochberg correction was used to compare multiple metabolite concentrations to keep the false discovery rate (FDR) <5%. Otherwise, the differences were considered significant at $P \leq 0.05$.

Multivariate analysis was first performed with SIMCA-P v.14.0 (Umetrics, Umea, Sweden), using principal component analysis (PCA) for detection of sample grouping and outliers. We then applied the least absolute shrinkage and selection operator (LASSO) method on mean centered-unit variance (MC-UV) scaled metabolites. With this method, a constraint or penalty is imposed on the coefficient of "classic" logistic regression to render the covariance matrix invertible; thus, enabling computation of the estimated variance of the regression coefficients.[15] This method is considered suitable for selection of variables, since some coefficients are "shrunk" toward exactly zero under the constraint. For the LASSO procedure, data were randomly split 1000 times into a training set containing approximately two-thirds of all data, obtained from 23 POAG patients and 18 controls, and a test set of data, obtained from 12 POAG patients and 9 controls. A LASSO model then was constructed for each iteration. Thus, we obtained 1000 estimations for the coefficients of each metabolite, and for the area calculated under the receiving operator characteristic curve (AUROC), for the training and test sets. The nullity of each coefficient then was tested using Student's *t*-test, and a "volcano" plot (coefficients versus *P* values) was constructed to highlight the most important metabolites. Since LASSO models using the whole set of metabolites might suffer from some degree of overfitting, we decided to integrate the most relevant metabolites shown by the volcano plot into a logistic regression (LR) model. Here again, the data were randomly split 1000 times into training and test sets, and the performance of the models was evaluated using the AUROC. Multivariate analysis was performed using the R packages glmnet,[16] glm, and ROCR packages (available in the public domain at http://www.Rproject.org).[17]

Results

Clinical Features of POAG Patients and Controls

Comparisons between individuals with POAG ($n = 36$) and controls ($n = 27$) in terms of demographic and environmental data, as well as comorbid medical conditions, are presented in Table 1. Mean age and sex ratios of individuals with POAG did not differ significantly from those of controls. There were no between-group differences regarding hypertension, hyperlipidemia, diabetes, or thyroid disease, but the body mass index (BMI) was significantly lower in individuals with POAG compared to the age- and sex-matched control group ($P < 0.01$; Table 1). There was no significant difference between the groups in term of systemic medications (Table 2).

The general ophthalmologic features of patients in the POAG and control groups also were compared (Table 3). Unsurprisingly, the POAG group had significantly thinner RNFL than controls as measured by OCT ($P < 0.001$). In contrast, there was no significant difference between the groups regarding IOP, which may have been affected by the treatment for glaucoma in the POAG group ($P = 0.60$) and the central corneal CCT ($P = 0.09$). Since the control group had received cataract surgery, visual acuity was significantly better than that in the POAG group ($P = 0.01$). In the POAG group, 50% had mild, 14% moderate, and 36% severe POAG.

Metabolomics Analysis

After validation of the kit plate based on QC samples, 37 (19.7%) metabolites were excluded because the measurements were not considered sufficiently accurate. Statistical analysis was then done on the remaining 151 (80.3%) metabolites (Supplementary Table S1).

Table 3. Ophthalmologic Features and Glaucoma Medication of Individuals With POAG Compared to Controls

	POAG ($N = 36$)	Controls ($N = 27$)	*P* Values
Mean visual acuity, LogMar	+0.12	+0.04	0.01*
Mean IOP, mm Hg	13.61	13.22	0.60
Mean CCT, μm	527	552	0.09
Average RNFL thickness, μm	65.27	87.00	<0.001*
Mean VF-MD, dB, worse eye	−7.84	–	–
Glaucoma severity, %			
Mild	50	–	–
Moderate	14	–	–
Severe	36	–	–
Glaucoma medications, %			
β-blockers	58	–	–
Prostaglandin analogue	64	–	–
α-2-agonists	8	–	–
Carbonic anhydrase inhibitor	30	–	–

* Statistically significant.

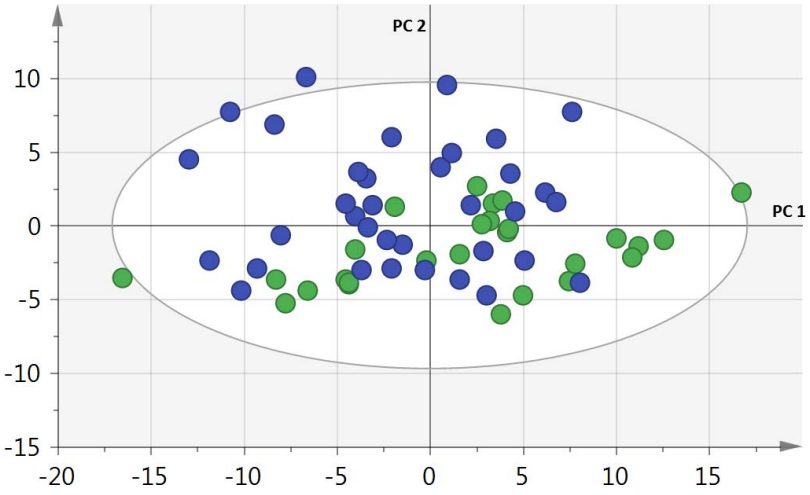

FIGURE 1. PCA scatter plot obtained from the matrix of metabolites for the 35 individuals suffering from glaucoma (*blue dots*) and 27 controls (*green dots*). There is no clear grouping of metabolites nor is there any outlier (according to Hotelling's T2 range). PC 1, 2, principal components 1 and 2.

The unsupervised PCA scatter plot of metabolomics data showed no grouping according to the POAG or control groups, nor any strong outliers in the first principal plan (PC1 versus PC2; Fig. 1).

After Benjamini-Hochberg correction, univariate analysis showed significant differences between the POAG and control groups for 13 metabolites, with a global false discovery rate (FDR) of 0.045 (Table 4).

The estimated mean coefficients and the $-\log_{10}(P$ values), that is the "volcano" plot, for the 1000 LASSO models obtained after randomly splitting the data set 1000 times into training and test sets are shown in Figure 2. Mean AUROC values for the training and test sets were 98.64% (95% confidence interval [CI], 98.34%–98.94%; $P < 2.2e\text{-}16$) and 81.16% (95% CI, 80.50–81.82; $P < 2.2e\text{-}16$), respectively (Supplementary Figs. S1A, S1B). Metabolites found important according to univariate analysis and/or multivariate analysis are shown in Figure 3.

The metabolites with the most important coefficients obtained with the LASSO method, that is, octadecadienyl-carnitine (C18:2), spermidine, decanoyl-carnitine (C10:1), and acyl-alkyl phosphatidylcholine 40:1 (PC ae 40:1; Fig. 2) were used for the logistic regression model. With the same 1000-time random splitting process as described above. Mean AUROC values for the logistic regression models predicting training and test set outcomes, that is glaucoma patients versus controls, were 95.71% (95% CI, 95.60%–95.83%; $P < 2.2e\text{-}16$) and 91.78% (95% CI, 91.41–92.15; $P < 2.2e\text{-}16$), respectively (Supplementary Figs. S1C, S1D).

The difference between the training and test set AUROC values for the LASSO (~17.5%) and logistic regression (~4%) models, and the better performances of the latter on the test sets (91.78 vs. 81.16%), are all indicative of a less over-fitted LR model compared to the LASSO models.

Of the total 188 metabolites analyzed, 151 were accurately measured in the plasma of individuals with POAG, and 18 showed significant differences of concentration compared to age- and sex-matched controls. With arrows (↑) and (↓) respectively indicating significantly increased and decreased metabolite concentrations in POAG patients compared to controls, univariate and multivariate analyses identified 7 of the 18 metabolites; that is, spermidine (↓), spermine (↓), octadecadienyl-carnitine (C18:2; ↓), tyrosine (↑), methionine (↑), the group of hexoses (↑), and the phosphatidylcholine acyl-alkyl 40:1 (PC ae 40:1; ↑). Six metabolites were identified by univariate analysis alone; that is, C18:1 octadecenoyl-carnitine (↓), methionine sulfoxide (MetSO; ↑), C3 propionyl-carnitine (↑), and the three phosphatidylcholines PC aa 34:2 (↑), PC aa 34:4 (↑), and PC aa 36:4 (↑); and five metabolites were identified by multivariate analysis alone; that is, C4 butyryl-carnitine (↑), C10:1 decenoyl-carnitine (↑), C12:1 dodecenoyl-carnitine (↑), arginine (↑), and histamine (↓).

DISCUSSION

Analysis of the 18 metabolites contributing to the POAG metabolomic signature points toward three main, closely associated pathophysiologic conditions: (1) faulty mitochondrial oxidation, (2) senescence-like metabolic alteration, and

TABLE 4. Univariate Analysis Showing the Significant Metabolites After Type I Error Correction

Metabolite	Fold Change (POAG/Control)	*P* Values	Corrected Threshold for Type I Error
Spermine	0.97	0.00035	0.00095
Octadecadienyl-carnitine, C18:2	0.82	0.00068	0.0015
Methionine sulfoxide	1.31	0.0013	0.0020
Tyrosine	1.25	0.0013	0.0024
Spermidine	0.90	0.0017	0.0029
Octadecenoyl-carnitine, C18:1	0.76	0.0017	0.0033
Methionine	1.27	0.0023	0.0038
Propionyl-carnitine, C3	1.30	0.0036	0.0042
Hexose	1.09	0.0041	0.0046
PC aa 34:2	1.15	0.0047	0.0050
PC aa 36:4	1.15	0.0048	0.0053
PC aa 34:4	1.22	0.0051	0.0057
PC ae 40:1	1.18	0.0053	0.0061

Fold changes were calculated using median values for the glaucoma and control groups. Diacyl and acyl-alkyl phosphatidylcholines are represented as PC aa X:Y and PC ae X:Y, respectively, where X represents the sum of the lengths of two alkyl chains, and Y the sum of the unsaturation in both chains.

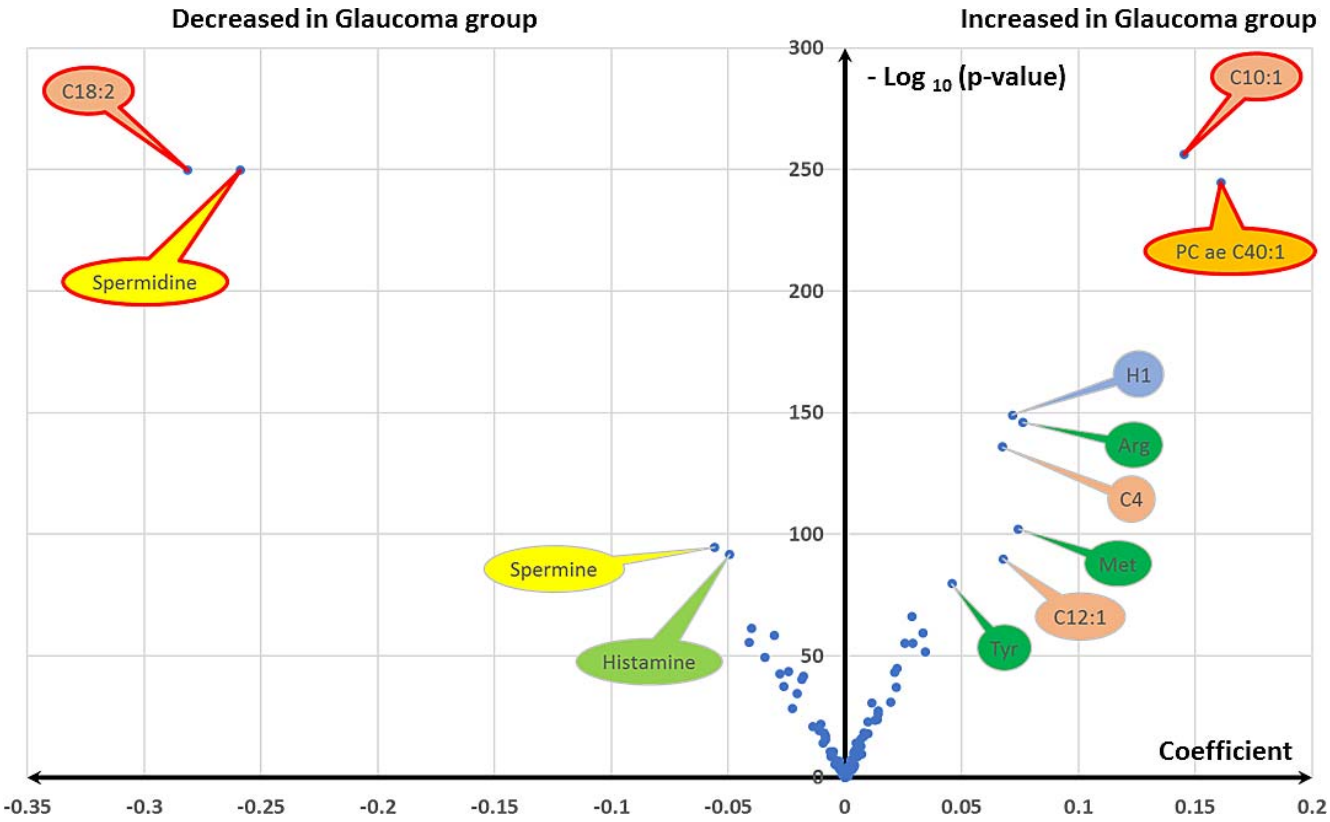

FIGURE 2. Volcano plot showing mean coefficient estimation for the 1000 LASSO models and $-\log_{10}$ (*P* value) obtained by testing the nullity of the mean of each of the 151 coefficients using this iterative process. Only the most important metabolites are labeled. Four metabolites, highlighted using a *red border*, are clearly distinguished from the other metabolites. Arg, arginine; Met, methionine; Tyr, tyrosine; H1, hexose; C4, butyryl-carnitine; C10:1, decenoyl-carnitine; C12:1, dodecenoyl-carnitine; C18:2, octadecadienyl-carnitine; PC ae 40:1, acyl-alkyl phosphatidylcholine 40:1.

(3) deficiency of molecules known to be protective for the retinal ganglion cells.

The hexoses, measured as a single group of metabolites in our study, were found at a significantly increased concentration (+9%) in the plasma of individuals with POAG compared to that of controls. Despite the frequent co-occurrence of diabetes and glaucoma, the increased concentration of hexoses could not be attributed either to diabetes or obesity in the individuals with POAG, who did not differ from the control population in terms of diagnoses of diabetes and antidiabetic medications. Moreover, the average BMI of individuals with POAG was significantly lower than that of controls. Our finding suggested a subtle systemic alteration of carbohydrate metabolism, perceptible in the blood, but that may have escaped detection by the two previous metabolomic studies performed on the blood of POAG[11] and PACG patients.[12] Interestingly, an inverse perturbation of carbohydrate metabolism has been reported in the aqueous humor of a rat model of glaucoma with a decreased concentration of glucose.[13]

The POAG signature also is characterized by modified concentrations of six acyl-carnitines. The concentrations of two short- (C3 and C4) and two medium- (C10:1 and C12:1) chain acyl-carnitines were increased, whereas the concentrations of two long-chain acyl-carnitines (C18:2 and C18:1) were decreased. This feature is in accordance with the two previous metabolomic studies that indicated a perturbation of the fatty acid metabolism. Burgess et al.[11] found only one acyl-carnitine, the long chain palmitoyl-carnitine, with an increased concentration in the POAG signature, whereas Rong et al.[12] found five discriminant long-chain free fatty acids; that is, palmitoleic (↑), linoleic (↓), γ-linoleic (↑), adrenic (↑), and arachidonic (↓) acids, but not the acyl-carnitines in their PACG patients. Mayordomo-Febrer et al.[13] also found increased free fatty acid concentrations in the aqueous humor of their rat model of glaucoma. Our approach allowed a complete overview of the acyl-carnitines that are involved in the mitochondrial mode of

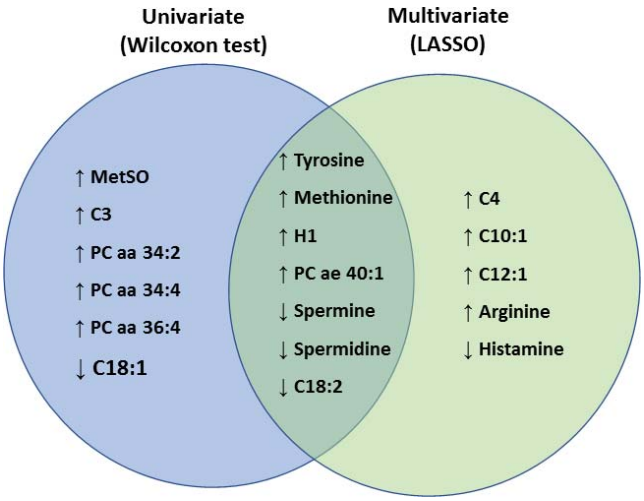

FIGURE 3. Venn diagram shows the most important metabolites found after univariate (*blue ellipse*) and multivariate (*green ellipse*) analyses. Metabolites with increased concentrations in the glaucoma group are represented by ↑, while those with diminished concentrations in this group are represented by ↓. C3, propionyl-carnitine; C18:1, octadecenoyl-carnitine; C18:2, octadecadienyl-carnitine; MetSO, methionine sulfoxide; PC aa 32:2, 34:4, 36:4, phosphatidylcholine diacyl 32:2, 34:4 and 36:4, respectively.

transport of fatty acids. An incomplete oxidation of fatty acids, leading to a reflux from mitochondria toward the blood of the smaller acyl-carnitines may be at the origin of the increased acyl-carnitine levels. Indeed, this phenomenon has been reported in inherited disorders of fatty acid oxidation.[18] In contrast the decreased concentration of the two-long chain acyl-carnitines that we observed is more likely to be involved in the senescence-like phenotype discussed below. In fact, the concentration of long-chain acyl-carnitines has been shown to decrease with age in the blood of mice.[19]

The increased concentration of the two main energetic suppliers represented by the sum of hexoses and acyl-carnitines argues strongly in favor of a generalized mitochondrial defect of oxidation. Several investigators have suggested that mitochondrial dysfunction contributes to glaucoma.[7,20,21] Comparison of the lymphoblasts of individuals with POAG with those of sex- and age-matched controls revealed a defect of complex I enzymatic activity (−18%) together with an impairment of complex I-related ATP synthesis (−19%), leading to the suggestion that POAG should be considered a true mitochondrial disease.[22,23] The energetic defect observed in lymphoblasts from POAG patients attests to the systemic character of mitochondrial impairment in the disease. The metabolomic signature we report concords with the notion of a subtle, generalized mitochondrial defect contributing to the pathogenesis of POAG. Considering the influence of the mitochondrial background on the BMI,[24–26] it is tempting to speculate that the significantly reduced BMI observed in the POAG group may be related to the weaker ability of mitochondria to oxidize energetic substrates.

Phosphatidylcholines are major phospholipids of cellular membranes. Accumulation of the four phosphatidylcholines found in our metabolomic signature has never before been reported in the blood of individuals with POAG to our knowledge. However, altered phosphatidylcholine profiles have been reported in the human glaucomatous trabecular meshwork[27] and aqueous humor.[28] The increased blood concentrations of phosphatidylcholine and particularly acyl-alkyl (ae) PC, which is of similar size, have been identified as biomarkers of senescence in the blood of mice.[29] Interestingly, PC ae 40:1, identified by univariate and multivariate analyses in our study as a key metabolite in POAG, has, in fact, already been patented as a biomarker of senescence (available in the public domain at http://www.google.sr/patents/WO2013139582A1?cl=en&hl=nl). In a metabolomics study performed in the plasma of 800 French volunteers, elderly healthy subjects had higher phosphatidylcholines plasma levels than young subjects.[30] Since our group of individuals with POAG did not differ significantly from controls in terms of age, it is tempting to speculate that the POAG-related mitochondrial dysfunction may lead to a biochemical phenotype of premature aging. Importantly, mitochondrial dysfunction recently has been shown to precede the onset of neurodegeneration of RGCs in a mouse model of glaucoma, mainly as a consequence of the age-related decrease in nicotinamide adenine dinucleotide (NAD), which is a key factor of mitochondrial energetic metabolism. Indeed, NAD supplementation by vitamin B3 has been shown to effectively prevent the occurrence of glaucoma in this model.[31] In this respect, the metabolomic profile of POAG that we have found should be a useful biomarker of vitamin B3 efficacy in clinical trials.

Concerning the pool of discriminant amino acids and biogenic amines, the most striking feature is the reduced concentration of spermidine and spermine in the POAG group compared to controls. Both of these metabolites are known to have an important role in optic nerves.[32] Spermidine mediates protection against oxidative damage and has a neuroprotective effect on RGCs after optic nerve injury in adult mice.[33] In a mouse model of normal-tension glaucoma, spermidine has been shown to prevent the neurodegeneration of RGCs.[34] Interestingly, Kim et al.[29] have reported decreased concentrations of spermidine and spermine in the blood of aged mice, as also found in several other organisms.[35] It is worth noting that methionine and arginine, which have increased concentrations in the metabolomic signature of POAG, are both precursors of the biosynthesis of spermidine and spermine, with methionine being a methyl radical donor. Thus, the senescence-related perturbation of spermidine and spermine biosynthesis may be involved in the accumulation of methionine and arginine. Spermidine and spermine also interact closely with mitochondria with regard to apoptosis and regulation of the mitochondrial membrane potential.[35] The significant decrease of spermidine and spermine we reported in the optic nerve of a mouse model of another form of optic neuropathy due to mutations in the *OPA1* gene, further illustrates the importance of these metabolites in optic nerve pathophysiology.[36] Thus, spermidine and spermine, which are related to mitochondrial dysfunction, senescence, and RGC damage, are central elements of the POAG signature. We were unable to explain the decreased concentration of histamine in POAG group compared to controls. However, the finding that histamine receptor antagonists induce or precipitate acute POAG[37] may suggest a possible causative relation. Nor were we able to explain the increased concentration of tyrosine in the blood of individuals with POAG. However, using the same approach of metabolomics in the exfoliation syndrome, the main cause of secondary glaucoma, we found a signature radically different from that of POAG, although both disease signatures shared similar variations of three metabolites; that is, spermidine, spermine and tyrosine, highlighting their importance as common pathophysiologic biomarkers.[38]

In conclusion, our standardized targeted metabolomics study, conducted on the plasma of individuals with POAG, revealed a comprehensive metabolic signature combining the accumulation of mitochondrial energetic substrates (sum of hexoses, short- and medium-chain acyl-carnitines) with senescence biomarkers (increased phosphatidylcholines and decreased spermine, spermidine, and long-chain acyl-carnitines), two of these metabolites; that is, spermidine and spermine, being known for their neuroprotective roles for RGCs. The presence of these circulating biomarkers in the blood of POAG patients reinforces the recent hypothesis of a generalized age-related systemic mitochondrial defect participating in the pathogenesis of POAG. Old age is a major risk factor of POAG and we know that the deficiency of neuroprotective polyamines is a cause of age-related RGC degeneration. Therefore, it is tempting to speculate that a premature mitochondrial dysfunction may augment the senescence phenotype, thus increasing the risk of POAG. Further work and replication by additional studies will be necessary to exhaustively decipher the metabolic contours of POAG and to identify the most pertinent clinical biomarkers of the disease.

Acknowledgments

The authors thank the individuals who participated in this study, Kanaya Malkani for critical reading and comments on the manuscript, and Odile Blanchet, MD, and the team of the Centre de Ressources Biologiques of the University Hospital of Angers for biobank sample processing.

Supported by Institut National de la Santé et de la Recherche Médicale (INSERM), Centre National de la Recherche Scientifique (CNRS), University of Angers, University Hospital of Angers, Région Pays de Loire and Angers Loire Métropole, and the following patients' associations: "Fondation VISIO," "Ouvrir les Yeux," "Union Nationale des Aveugles et Déficients Visuels,"

"Association contre les Maladies Mitochondriales," "Retina France," "Kjer France," "Fondation Berthe Fouassier," "Fondation pour la Recherche Médicale," and "Association Point de Mire."

Disclosure: **S. Leruez**, None; **A. Marill**, None; **T. Bresson**, None; **G. de Saint Martin**, None; **A. Buisset**, None; **J. Muller**, None; **L. Tessier**, None; **C. Gadras**, None; **C. Verny**, None; **P. Gohier**, None; **P. Amati-Bonneau**, None; **G. Lenaers**, None; **D. Bonneau**, None; **G. Simard**, None; **D. Milea**, None; **V. Procaccio**, None; **P. Reynier**, None; **J.M. Chao de la Barca**, None

References

1. Jonas JB, Aung T, Bourne RR, et al. Glaucoma. *Lancet*. 2017; 390:2183–2193.
2. Quigley HA, Broman AT. The number of people with glaucoma worldwide in 2010 and 2020. *Br J Ophthalmol*. 2006;90:262–267.
3. Stevens GA, White RA, Flaxman SR, et al.; Vision Loss Expert Group. Global prevalence of vision impairment and blindness: magnitude and temporal trends, 1990-2010. *Ophthalmology*. 2013;120:2377–2384.
4. Tham YC, Li X, Wong TY, et al. Global prevalence of glaucoma and projections of glaucoma burden through 2040: a systematic review and meta-analysis. *Ophthalmology*. 2014; 121:2081–2090.
5. Weinreb RN, Khaw PT. Primary open-angle glaucoma. *Lancet*. 2004;363:1711–1720.
6. Kamel K, Farrell M, O'Brien C. Mitochondrial dysfunction in ocular disease: focus on glaucoma. *Mitochondrion*. 2017;35: 44–53.
7. Inman DM, Harun-Or-Rashid M. Metabolic vulnerability in the neurodegenerative disease glaucoma. *Front Neurosci*. 2017; 11:146.
8. Tan SZ, Begley P, Mullard G, et al. Introduction to metabolomics and its applications in ophthalmology. *Eye (Lond)*. 2016;30:773–783.
9. Lauwen S, de Jong EK, Lefeber DJ, den Hollander Al. Omics biomarkers in ophthalmology. *Invest Ophthalmol Vis Sci*. 2017;58:BIO88–BIO98.
10. Barbosa-Breda J, Himmelreich U, Ghesquière B, et al. Clinical metabolomics and glaucoma. *Ophthalmic Res*. 2018;59:1–6.
11. Burgess LG, Uppal K, Walker DI, et al. Metabolome-wide association study of primary open angle glaucoma. *Invest Ophthalmol Vis Sci*. 2015;56:5020–5028.
12. Rong S, Li Y, Guan Y, et al. Long-chain unsaturated fatty acids as possible important metabolites for primary angle-closure glaucoma based on targeted metabolomic analysis. *Biomed Chromatogr*. 2017;31:e3963.
13. Mayordomo-Febrer A, López-Murcia M, Morales-Tatay JM, et al. Metabolomics of the aqueous humor in the rat glaucoma model induced by a series of intracamerular sodium hyaluronate injection. *Exp Eye Res*. 2015;131:84–92.
14. Weinreb RN, Friedman DS, Fechtner RD, et al. Risk assessment in the management of patients with ocular hypertension. *Am J Ophthalmol*. 2004;138:458–467.
15. Tibshirani R. Regression shrinkage and selection via the lasso. *J R Stat Soc Ser B*. 1996;58:267–288.
16. Friedman J, Hastie T, Tibshirani R. Regularization paths for generalized linear models via coordinate descent. *J Stat Softw*. 2010;33:1–22.
17. Sing T, Sander O, Beerenwinkel N, Lengauer T. ROCR: visualizing classifier performance in R. *Bioinformatics* 2005; 21:3940–3941.
18. Rinaldo P, Cowan TM, Matern D. Acylcarnitine profile analysis. *Genet Med*. 2008;10:151–156.
19. Houtkooper RH, Argmann C, Houten SM, et al. The metabolic footprint of aging in mice. *Sci Rep*. 2011;1:134.
20. Lee S, Van Bergen NJ, Kong GY, et al. Mitochondrial dysfunction in glaucoma and emerging bioenergetic therapies. *Exp Eye Res*. 2011;93:204–212.
21. Osborne NN, Núñez-Álvarez C, Joglar B, Del Olmo-Aguado S. Glaucoma: focus on mitochondria in relation to pathogenesis and neuroprotection. *Eur J Pharmacol*. 2016;787:127–133.
22. Lee S, Sheck L, Crowston JG, et al. Impaired complex-I-linked respiration and ATP synthesis in primary open-angle glaucoma patient lymphoblasts. *Invest Ophthalmol Vis Sci*. 2012;53: 2431–2437.
23. Van Bergen NJ, Crowston JG, Craig JE, et al. Measurement of systemic mitochondrial function in advanced primary open-angle glaucoma and Leber hereditary optic neuropathy. *PLoS One*. 2015;10:e0140919.
24. Wortmann SB, Zweers-van Essen H, Rodenburg RJ, et al. Mitochondrial energy production correlates with the age-related BMI. *Pediatr Res*. 2009;65:103–108.
25. Yang TL, Guo Y, Shen H, et al. Genetic association study of common mitochondrial variants on body fat mass. *PLoS One*. 2011;6:e21595.
26. Bharadwaj MS, Tyrrell DJ, Leng I, et al. Relationships between mitochondrial content and bioenergetics with obesity, body composition and fat distribution in healthy older adults. *BMC Obes*. 2015;2:40.
27. Aribindi K, Guerra Y, Lee RK, Bhattacharya SK. Comparative phospholipid profiles of control and glaucomatous human trabecular meshwork. *Invest Ophthalmol Vis Sci*. 2013;54: 3037–3044.
28. Edwards G, Aribindi K, Guerra Y, et al. Phospholipid profiles of control and glaucomatous human aqueous humor. *Biochimie*. 2014;101:232–247.
29. Kim S, Cheon HS, Song JC, et al. Aging-related changes in mouse serum glycerophospholipid profiles. *Osong Public Health Res Perspect*. 2014;5:345–350.
30. Trabado S, Al-Salameh A, Croixmarie V, et al. The human plasma-metabolome: reference values in 800 French healthy volunteers; impact of cholesterol, gender and age. *PLoS One*. 2017;12:e0173615.
31. Williams PA, Harder JM, Foxworth NE, et al. Vitamin B 3 modulates mitochondrial vulnerability and prevents glaucoma in aged mice. *Science*. 2017;355:756–760.
32. Ingoglia NA, Sturman JA, Eisner RA. Axonal transport of putrescine, spermidine and spermine in normal and regenerating goldfish optic nerves. *Brain Res*. 1977;130:433–445.
33. Noro T, Namekata K, Kimura A, et al. Spermidine promotes retinal ganglion cell survival and optic nerve regeneration in adult mice following optic nerve injury. *Cell Death Dis*. 2015a;6:e1720.
34. Noro T, Namekata K, Azuchi Y, et al. Spermidine ameliorates neurodegeneration in a mouse model of normal tension glaucoma. *Invest Ophthalmol Vis Sci*. 2015;56:5012–5019.
35. Minois N, Carmona-Gutierrez D, Madeo F. Polyamines in aging and disease. *Aging*. 2011;3:716–732.
36. Chao de la Barca JM, Simard G, Sarzi E, et al. Targeted metabolomics reveals early dominant optic atrophy signature in optic nerves of *Opa1*$^{delTTAG/+}$ mice. *Invest Ophthalmol Vis Sci*. 2017;58:812–820.
37. Tripathi RC, Tripathi BJ, Haggerty C. Drug-induced glaucomas: mechanism and management. *Drug Saf*. 2003;26:749–767.
38. Leruez S, Bresson T, Chao de la Barca JM, et al. A plasma metabolomic signature of the exfoliation syndrome involves amino acids, acylcarnitines, and polyamines. *Invest Ophthalmol Vis Sci*. 2018;59:1025–1032.

Investigative Ophthalmology & Visual Science